第 29 卷第 3 期
2010 年 6 月

红 外 与 毫 米 波 学 报
J. Infrared Millim. Waves

Vol. 29, No. 3
June,2010

文章编号:1001 - 9014(2010)03 - 0167 - 05

OPTICAL PROPERTIES OF COLLOIDAL CdSe TETRAPOD NANOCRYSTALS

ZHAO Li-Juan[1,2], Pang Qi[2], YANG Shi-He[3], GE Wei-Kun[2], WANG Jian-Nong[2]

(1. Applied Physics Department, Donghua University, Shanghai 201620, China;
2. Physics Department and the Institute of Nano-Science and Technology, Hong Kong University of Science and Technology, Clear Water Bay, Hong Kong, China;
3. Chemistry Department and the Institute of Nano-Science and Technology, Hong Kong University of Science and Technology, Clear Water Bay, Hong Kong, China)

Abstract: Time resolved optical properties of CdSe tetrapod nanocrystals where studied. The results show that the decays of photoluminescence (PL) intensities for tetrapods in solution and on insulating silicon substrate can be well fitted by a bi-exponential function. Based on the emission-energy dependence of carrier lifetimes, the fast and slow PL decays of CdSe tetrapods are attributed to the recombination of delocalized carriers and the localized carriers in the localized states, respectively. By comparing the amplitude ratio of the fast-decay component to the slow-decay component for samples in solution with those on silicon, it is concluded that the slow PL decay is associated with the recombination of localized carriers in the surface defects of CdSe tetrapods.

Key words: tetrapod nanoparticle; decay of photoluminescence; localized carrier; surface defect
CLC number: 0433.1; 0472 + .3; 0482.31 **Document**: A

CdSe 四脚状纳米颗粒的光学性质

赵莉娟[1,2], 庞 起[2], 杨世和[3], 葛惟昆[2], 王建农[2]

(1. 东华大学 应用物理系,上海 201620;2. 香港科技大学 物理系及香港科技大学纳米研究所,香港;
3. 香港科技大学 化学系及香港科技大学纳米研究所,香港)

摘要:主要研究了高产率 CdSe 四脚状纳米颗粒的时间分辨光学性质. 结果表明在氯仿溶液中和均匀涂布在绝缘硅片上的 CdSe 四脚状纳米颗粒室温下的光致发光(PL)衰减曲线均可以用一个双 e 指数的衰减函数来拟合,荧光寿命短的部分对应快衰减,而寿命长的部分对应慢衰减. 通过分析荧光寿命与 PL 峰的能量的关系可知,快衰减和慢衰减分别来自于非局域态载流子和局域态载流子的贡献. 通过比较溶液中和硅片上两种情况的快衰减和慢衰减系数的比值,得出结论:CdSe 四脚状纳米颗粒的 PL 快衰减和慢衰减分别来源于纳米颗粒中非局域态和颗粒表面缺陷中局域态的贡献.

关 键 词:四脚状纳米颗粒;PL 衰减;局域载流子;表面缺陷

Introduction

The size and shape of semiconductor nanostructures play important roles that determine their electronic and optical properties. The tetrapod-shaped nanocrystals have attracted much attention these years. They can potentially lead to a variety of interesting mechanical, electrical, and optical properties. For example, due to their three-dimensional character, tetrapods may be important alternatives to fibers and rods as additives for mechanical reinforcement of polymers [1]. Tetrapods can also serve as a very interesting building

Received date: 2009 - 01 - 13, **revised date**: 2010 - 03 - 01 **收稿日期**:2009 - 01 - 13, **修回日期**:2010 - 03 - 01
Foudantion item: Supported by the Research Grant Council of Hong Kong(HKUST6069/02P, F-HK18/03T) and the research fund of Donghua University
Biography: ZHAO Li-Juan(1978-), female, Guizhou, China, lecturer of Donghua University, research fields are syntheses, optical and electrical properties of semiconductor nano materials, and the corresponding semiconductor devices.

block for preparing superstructures, especially three-dimensional ones[2]. Three-dimensional CdSe tetrapods have obvious potential advantages in photovoltaic devices[3,4] because their shape makes it impossible for them to lie flat within the film. One important concern in these applications is the dynamic properties of luminescence from tetrapods, which not only help to gain fundamental insight into the charge carrier properties but also provide information to improve the luminescence yield. Up to now, tetrapods-shaped crystals with dimensions on the nanometer and micrometer scale have been synthesized for a variety of II-VI semiconductors including ZnO[5,6], CdS[7~9], CdTe[1,10] and CdSe[11,12]. The mechanical, electrical and optical properties of these tetrapod-shaped semiconductor nanocrystals were also investigated by several groups[12~17]. However, up to now, the recombination dynamics of luminescerce in colloidal CdSe tetrapod nanocrystals have rarely been reported.

Here we focus on the investigations of the recombination dynamics of CdSe tetrapod nanocrystals. Time-resolved photoluminescence (PL) decay measurements have been carried out at room temperature for the CdSe tetrapod-shaped nanocrystals in air (on insulating silicon substrate) and in chloroform solution at various emission wavelengths. The PL intensity shows a bi-exponential decay, consisting of a fast component (0.92 ns and 0.84 ns for tetrapods in solution and on silicon, respectively) and a slow component (12.80 ns and 7.19 ns for tetrapods in solution and on silicon, respectively). The nature of PL in our CdSe tetrapods is discussed.

1 Experimental details

The detailed synthesis procedure of colloidal CdSe tetrapod-shaped nanocrystals can be found elsewhere[15]. A brief description of the synthesis is presented below. Selenium powder was dissolved in TOP. The mixture of CdO, oleic acid (OA), diphenyl ether and HCl (37%, aqueous solution) were heated to 180℃ for 2 hours under N_2 gas flow. The addition of HCl is for the formation of tetrapods[15]. Then the solution of selenium powder and TOP was quickly injected into this mixture. The reaction temperature remained to be 180℃. After 1 hour, an aliquot was taken out from the reaction flask and quickly transferred into a vial filled with chloroform. The obtained crude sample was washed by methanol. After centrifugal separation, the precipitate can be separated from the excess OA and reactants. Afterwards the nanocrystals were re-dispersed into chloroform forming clear and red solution.

PL time-resolved measurements were performed using the time-resolved confocal fluorescence spectroscopy system. The excitation source is the second-harmonic generation of a tunable femtosecond Ti:sappire laser (Mira900-F, Coherent) at a wavelength of 400 nm. The Ti:sappire laser produces light pulses with 200 fs duration and a repetition rate of 10 MHz. To reduce photo bleaching, the excitation power on samples was controlled below 100 μW, and the accumulation time was set to 30 s to produce high-quality signals at each wavelength band. A water immersion objective lens (40 × and NA = 1.15) focuses the excitation beam into the samples and collects the backscattered fluorescence signals. A pair of galvomirrors scans the laser beam and creates a 150μm × 150μm sampling area in the sample. A 200μm core optical fiber is used as a pinhole to collect the confocal fluorescence and conduct the signal to a spectrometer. The detector is a multichannel time-correlated single-photon-counting (TCSPC) module (SPC-730 and PML-16, Becker & Hickl GmbH) with a linear array of 16 photomultiplier tubes (PMTs) that record fluorescence signals in 16 spectral bands from 470 to 670 nm with a 13 nm interval. The instrument responses of all PMT channels have ~180 ps FWHM. There are no significant temporal shifts between the separate channels. The recorded signal is the averaged fluorescence over the sampling area (150μm × 150μm) to minimize the heterogeneity of intracellular fluorescence [18~20].

2 Results and discussions

Transmission electron microscopy (TEM) images show that the tetrapod yield is up to 80%[15]. High resolution TEM (HRTEM) images indicate that the average size of the core of tetrapods is about 4nm, the widths of the tetrapods' arms are about 4 nm, and the lengths of the arms are about 8 nm. Fig. 1 (a) and

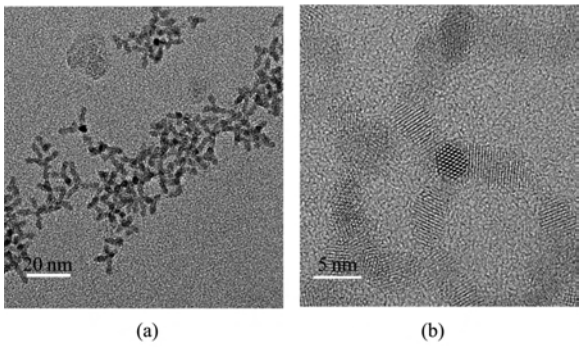

Fig. 1　Representative TEM image (a) and high resolution TEM image (b) of CdSe tetrapod-shaped nanocrystals
图 1　CdSe 四脚状纳米晶粒的 (a)低倍透射电镜(b)高分辨透射电镜图

(b) illustrate the representative TEM and HRTEM images of the synthesized CdSe, respectively.

The room-temperature PL spectra have been obtained from the samples in chloroform solution and the samples deposited on insulating silicon substrates. The dashed lines in Fig. 2 are the PL signals of CdSe tetrapods in chloroform solution (a) and on silicon substrate (b) at room temperature. The energy of the main peak is centered at 2.20 eV and 2.16 eV for tetrapods in solution and on silicon, respectively, which is assigned to the recombination of near-bandgap excitons from the UV-Vis absorption spectra of samples. The energy difference between the main PL peaks of samples in solution and on silicon can be explained as follows. Due to the gravity, larger-sized samples in solution prefer to stay at the bottom of the vessel [21]. While in the measurements of PL emissions from samples in solution, the illuminated points are in the middle of the vessel. Therefore, the average size of samples in solution is smaller than that of samples on silicon, i. e. the emission energy of samples in solution is higher than that of samples on silicon. Fig. 3 shows the PL decay profiles of tetrapods in solution (a) and on silicon (b) monitored at the PL peak energies (2.20 eV and 2.16 eV). The decay can be well fitted by a bi-exponential function

$$I(t) = A_1 e^{-\frac{t}{\tau_1}} + A_2 e^{-\frac{t}{\tau_2}} \quad , \qquad (1)$$

where τ_1 (τ_2) represents the decay time of fast (slow) decay; A_1 (A_2) represents the amplitude of the fast-decay (slow-decay) component at $t = 0$. The solid lines in Fig. 3 are the fitted results by using Equation (1).

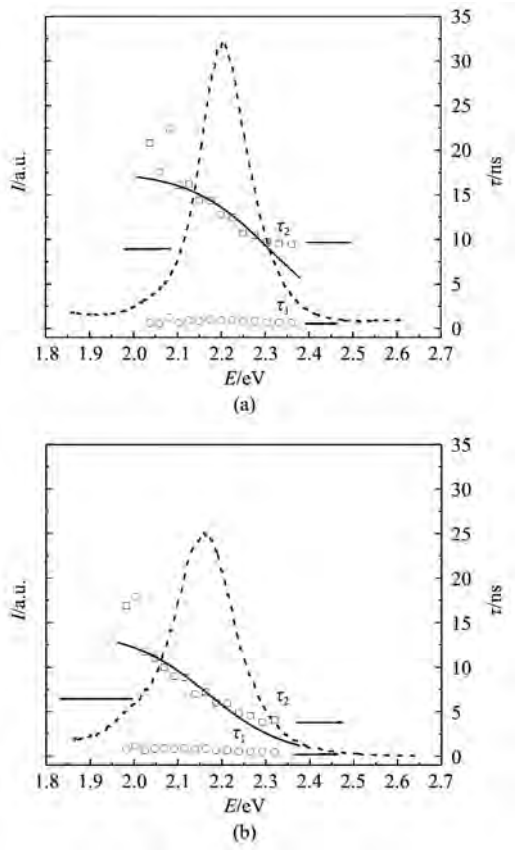

Fig. 2　The PL spectra (*I-E* curves) (dashed lines) of CdSe tetrapods in solution (a) and on silicon (b) at room temperature, respectively. The open circles and squares show emission energy dependence of τ_1 and τ_2 (τ-*E* curves), respectively. The solid lines are the fitting results by using equation (2)
图 2　溶液中(a)和硅片上(b)的 CdSe 四脚状纳米晶的室温 PL 曲线 (*I-E* 曲线)(虚线所示). 空心圆和空心正方形所示分别为衰减时间常数 τ_1 和 τ_2 与 PL 能量之间的关系 (τ-*E* 曲线),实线为用方程(2)拟合的结果)

As can be seen, an excellent agreement with experimental results can be achieved. The decay fittings give time constants of $\tau_1 = 0.92$ ns and 0.84 ns for fast PL decay and $\tau_2 = 12.80$ ns and 7.19 ns for slow PL decay for tetrapods in solution and on silicon, respectively.

To investigate the origins of τ_1 and τ_2, their dependences on emission energy are analyzed as shown in Fig. 2. The open circles and squares in Fig. 2 (a) show the measured lifetimes of slow (τ_2) and fast (τ_1) decay, respectively, for different emission energy for CdSe tetrapods in solution. As shown in Fig. 2 (a), the lifetime τ_2 falls as the emission energy increases. It is a characteristic of the localization effect[22~24]. Localization associated with the structural disorder or surface states may generate localized states

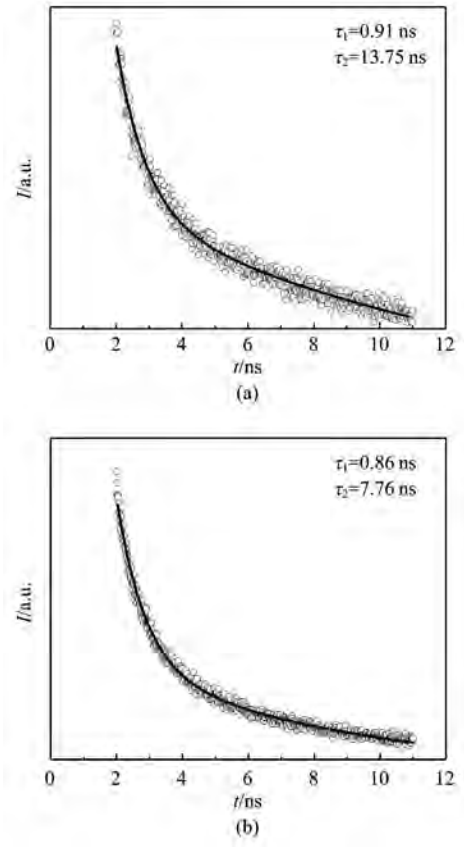

Fig. 3 The room temperature PL decay profiles of CdSe tetrapods in solution (a) and on silicon (b), respectively, monitored at peak transitions (2.20 eV and 2.16 eV for tetrapods in solution and on silicon, respectively) (*I-t* curves). The solid lines are fitting results by using equation (1)
图3 溶液中(a)和硅片上(b)的 CdSe 四脚状纳米晶在 PL 峰附近的室温 PL 衰减曲线 (*I-t* 曲线). 实线为用方程(1)拟合的结果)

with different energies [25]. Accordingly, localized carriers can be transferred from higher energy sites to lower energy sites through a relaxation process[24]. The decay rate of localized carriers is expressed as the radiative recombination rate plus the transfer rate to lower energy sites, where the radiative recombination rate is assumed to be independent on emission energy. Thus, the observed lifetime decreases as the emission energy increases. While the fast PL decay τ_1 is independent on emission energy (as shown in Fig. 2 (a)) and much shorter than τ_2, these suggest that τ_1 is associated with the recombination of delocalized carriers in the core state in tetrapods[21]. Fig. 2(b) shows that the measured lifetimes of slow and fast decay for different emission energies for the tetrapods on silicon have the same characteristics as that for tetrapods in solution, i.e. τ_1 is independent on emission energy, while τ_2 decreases as emission energy increases. The combination of carrier recombination and transfer has been modeled by assuming that the density of localized tail states is proportional to $\exp(-E/E_0)$, where E_0 describes the amount of spreading in the density of states[24, 26]. The relationship between lifetime $\tau(E)$ and PL energy E is given as [26]

$$\tau(E) = \frac{\tau_{rad}}{1 + \exp[(E - E_{me})/E_0]}, \qquad (2)$$

where τ_{rad} is the radiative lifetime, E_{me} is defined as the energy for which the decay time equals to the transfer time, and E_0 is a characteristic energy for the density of states. The latter parameter is a measure for the average localization energy. When PL emission energies are above E_{me}, the transfer of carriers has a higher probability than the radiative decay. Fig. 2 shows the fitted curves to Equation (2) (solid line in Fig. 2). PL decay signals at lower and higher energies are much weak, so that τ_1 and τ_2 at lower and higher energies are least-square fits of Eq. (1), which can explain the divergence between the fitted curves and the experimental data at lower and higher energy. But as showed in Fig. 2, $\tau_2 - E$ curves can be well fitted by Eq. (2) when the energy ranges from 2.03 eV to 2.26 eV, which indicates further that the slow decay is related with the recombination of carriers in localized states of the tetrapods.

From the PL decay fittings, the amplitude ratio of the fast-decay component A_1 to the slow-decay component A_2 can be analyzed to explore further the origins of the fast and slow PL decays. The ratio A_1/A_2 is smaller than 1 for tetrapods in solution (1/1.48 for peak energy), while larger than 1 for tetrapods on silicon (1.79/1 for peak energy) for all emission energies, indicating that for tetrapods in solution the weight of slow decay which is characterized by a localization process is lager than that of fast decay, while the reverse is true for tetrapods on silicon. Note that the only difference between tetrapods in solution and on silicon is the external environment. For tetrapods in chloroform solution, the tetrapods are in a non-polar environment, while for tetrapods on silicon, the tetrapods are exposed to air which contains oxygen, water molecule, and etc. Air

表 1　Summary of fitting parameters for PL decays at peak energies

Table 1　PL 衰减曲线在峰能量附近的拟合结果

Samples		PL peak (eV)	τ_1 (ns)	τ_2 (ns)	A_1/A_2	τ_{rad} (ns)	E_{me} (eV)	E_0 (meV)
CdSe	In solution	2.20	0.92	12.8	1/1.48	17.6	2.31	91
Tetrapods	On silicon	2.16	0.84	7.19	1.79/1	14	2.17	88

is a polar atmosphere and oxygen can be absorbed on the surface of tetrapods to eliminate the polar surface defects such as defects formed by Se/Cd dangling bonds[22]. Therefore, for tetrapods on silicon the weight of fast decay is lager than that of slow decay and it is believed that the slow-decay component originates from the recombination of localized carriers in the surface states.

The fitting parameters for PL decays of CdSe tetrapods are summarized in Table 1.

3　Conclusions

In summary, the recombination dynamics of photoluminescence for colloidal CdSe tetrapods were studied. Based on the emission energy dependence of lifetimes and the amplitude ratio A_1/A_2, it is believed that the fast and slow PL decay of colloidal CdSe tetrapods are associated with the recombination of the delocalized carriers in the core states and the localized carriers in the surface states, respectively. This important result not only helps to gain fundamental insight into the charge carrier properties of CdSe tetrapod-shaped nanocrystals, but also provides information to improve the luminescence yield of the tetrapods.

Acknowledgement: The authors would like to thank Mr. Zheng Wei of ECE Department of HKUST for the measurements of lifetimes and the financial support of the Research Grant Council of Hong Kong via grant number HKUST6069/02P and F-HK18/03T, and the research fund of Donghua University.

REFERENCES

[1] Manna L, Milliron D J, Meisel A, *et al*. Controlled growth of tetrapod-branched inorganic nanocrystals[J]. *Nat. Mater*, 2003, **2**: 382—385.

[2] Liu H T, Alivisatos A P. Preparation of asymmetric nanostructures through site selective modification of tetrapods [J]. *Nano Lett*. 2004, **4**: 2397—2401.

[3] Sun B Q, Marx E, Greenham N C. Photovoltaic devices using blends of branched CdSe nanoparticles and conjugated polymers[J]. *Nano Lett*. 2003, **3**: 961—963.

[4] Scher E C, Manna L, Alivisatos A P. Shape control and applications of nanocrystals[J]. *Philos. Trans. R. Soc. London, Ser. A* 2003, **361**: 241—257.

[5] Dai Y, Zhang Y, Li Q K, *et al*. Synthesis and optical properties of tetrapod-Like zinc oxide nanorods [J]. *Chem. Phys. Lett*. 2002, **358**: 83—86.

[6] Yan H Q, He R, Pham J, *et al*. Morphogenesis of one-dimensional ZnO nano-and microcrystals [J]. *Adv. Mater*. 2003, **15**: 402—405.

[7] Jun Y W, Lee S M, Kang N J, *et al*. Controlled synthesis of multi-armed CdS nanorod architectures using monosurfactant system [J]. *J. Am. Chem. Soc*. 2001, **123**: 5150—5151.

[8] Jun Y W, Jung Y Y, Cheon J. Architectural control of magnetic semiconductor nanocrystals[J]. *J. Am. Chem. Soc*. 2002, **124**: 615—619.

[9] Chen M, Xie Y, Lu J, *et al*. Synthesis of rod-, twinrod-, and tetrapod-shaped CdS nanocrystals using a highly oriented solvothermal recrystallization technique[J]. *J. Mater. Chem*. 2002, **12**: 748—753.

[10] Yu W W, Wang Y A, Peng X G. Controlled CdTe nanocrystals: Ligand effects on monomers and nanocrystals[J]. *Chem. Mater*. 2003, **15**: 4300—4308.

[11] Peng A, Peng X G. Nearly monodisperse and shape-controlled CdSe nanocrystals via alternative routes: Nucleation and growth [J]. *J. Am. Chem. Soc*. 2002, **124**: 3343—3353.

[12] Manna L, Scher E C, Alivisatos A P. Synthesis of soluble and processable rod-, arrow-, teardrop-, and tetrapod-shaped CdSe nanocrystals[J]. *J. Am. Chem. Soc*. 2000, **122**: 12700—12706.

[13] Peng X, Manna L, Yang W, *et al*. Shape control of CdSe nanocrystals[J]. *Nature* 2000, **404**: 59—61.

[14] Fang L, Park J Y, Cui Y, *et al*. Mechanical and electrical properties of CdTe tetrapods studied by atomic force microscopy [J]. *J. Chem. Phys*. 2007, **127**: 184704—184708.

[15] Pang Q, Zhao L J, Cai Y, *et al*. CdSe nano-tetrapods: controllable synthesis, structure analysis, and electronic and optical properties[J]. *Chem. Mater*. 2005, **17**: 5263—5267.

[16] Li Y, Zhong H, Li R, *et al*. High-yield fabrication and electrochemical characterization of tetrapodal CdSe, CdTe, and $CdSe_xTe$ [J]. *Adv. Funct. Mater*. 2006, **16**: 1705—1716.

[17] Malkmus S, Kudera S, Manna L, *et al*. Electron-hole dynamics in CdTe tetrapods [J]. *J. Phys. Chem. B*2006, **110**: 17334—17338.

[18] Wu Y, Xi P, Chueng T, *et al*. Depth-resolved fluorescence spectroscopy reveals layered structure of tissue[J]. *Opt. Express* 2004, **12**: 3218—3223.

[19] Wu Y, Xi P, Chueng T, *et al*. Depth-resolved fluorescence spectroscopy of normal and dysplatic cervical tissue [J]. *Opt. Express* 2005, **13**: 382—388.

[20] Wu Y, Zheng W, Qu J. Sensing cell metabolism by time-resolved autofluorescence [J]. *Opt. Lett*. 2006, **31**: 3122—3124.

[21] Guo B. Chemical synthesis and characterization of CdMnS and CdMnSe quantum dots[D]. Hong Kong University of Science and Technology, MPhil Thesis 2003: 52—53.

(下转第 179 页)

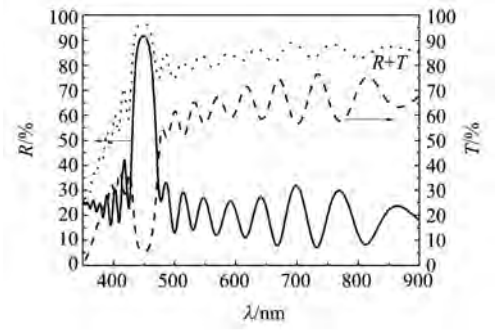

图 4　FTO/ $PbZr_{0.4}Ti_{0.6}O_3$-多层膜系统的反射和透射光谱. 实线对应反射曲线,虚线对应透射谱,点线代表反射率和透射率之和

Fig. 4　Reflectance and transmittance spectra of the FTO/ PZT multilayer, the solid line corresponds to the reflectance spectra, and the dashed line to the transmittance spectra, respectively, while the dotted line denotes the sum of the reflectance and the transmittance spectra

射特性;同时也说明 FTO/PZT 多层膜系统以透射方式工作时,可以用作滤光片. 另外,注意到图 4 中 FTO/PZT 多层膜系的反射率 R 与透射率 T 之和 $R+T$,在整个测量范围 $R+T$ 均小于 1,说明整个膜系依然存在与波长相关的光学吸收与散射.

3　结论

用溶胶 – 凝胶工艺在涂布 SnO_2:F 的玻璃衬底上制备了高质量、拥有 16 个周期的 $PbZr_{0.4}Ti_{0.6}O_3$ 多层膜. $PbZr_{0.4}Ti_{0.6}O_3$ 薄膜不仅具有均匀致密的表面形貌,而且呈现出由致密层和多孔层交替排列形成的层状结构. X 射线衍射数据显示,$PbZr_{0.4}Ti_{0.6}O_3$ 薄膜已完全转化成单一的钙钛矿相. 反射与透射光谱的测量结果则表明,FTO/PZT 多层膜系统具有作为一维光子晶体的良好性能. 本研究对进一步促进铁电材料在光子带隙工程领域的应用将有积极意义.

REFERENCES

[1] ZHANG Fu-Xue, WANG Li-Kun. *Modern Piezoelectricity* [M]. Volume 2. Beijing: Science Press(张福学,王丽坤. **现代压电学(中册)**. 北京:科学出版社),2002,233.

[2] Scott J F, Araujo. Ferroelectric memories[J]. *Science*, 1989,**246**:1400—1405.

[3] Whatmore R W, Osbond P C, Shorrocks N M. Ferroelectric materials for thermal IR detectors[J]. *Ferroelectrics*,1987, **76**:351—367.

[4] Zhu Sh N, Zhu Y Y, Ming N B. Quasi-phase-matched third-harmonic generation in a quasi-periodic optical superlattice[J]. *Science*,1997,**278**:843—846.

[5] Hu Gu-Jin, Chen Jing, An D L, *et al.* Fabrication of ferroelectric $PbZr_{0.4}Ti_{0.6}O_3$ multilayers by sol-gel process[J]. *Appl. Phys. Lett.*,2005,**86**:162905.

[6] Hong Xue-Kun, Hu Gu-Jin, Chen Jing, *et al.* $Ba_{0.9}Sr_{0.1}TiO_3$-based Bragg reflectors fabricated from one single chemical solution [J]. *Appl. Phys. Lett.*, 2006, **89**: 082902.

[7] Hong Xue-Kun, Hu Gu-Jin, Shang Jing-Lin, *et al.* $Ba_{0.9}Sr_{0.1}TiO_3$-based optical microcavities fabricated by chemical solution deposition [J]. *Appl. Phys. Lett.*, 2007, **90**: 251911—251914.

[8] HU Gu-Jin, HONG Xue-Kun, CHEN Jing, *et al.* Formation mechanism of periodical ferroelectric multilayers with high optical reflectivity[J]. *J. Infrared Millim. Waves*(胡古今,洪学鹃,陈静,等. 高反射率周期性铁电多层膜形成机理研究. **红外与毫米波学报**),2007,**26**(2):89—91.

[9] Hu Gu-Jin, Hong Xue-Kun, Chu Jun-Hao, *et al.* Ferroelectric and optical properties of quasiperiodic $PbZr_{0.5}Ti_{0.5}O_3$ multilayers grown on quartz wafers[J]. *Appl. Phys. Lett.*, 2007,**90**:162904.

[10] Takenaka Shinsuke, Kozuka Hiromitsu. Sol-gel preparation of single-layer, 0.75μm thick lead zirconate titanate films from lead nitrate-titanium and zirconium alkoxide solutions containing polyvinylpyrrolidone[J]. *Appl. Phys. Lett.*,2001,**79**:3485—3487.

[11] Osone S, Brinkman K, Shinmojo Y, *et al.* Ferroelectric and piezoelectric properties of $Pb(Zr_xTi_{1-x})O_3$ thick films prepared by chemical solution deposition process[J]. *Thin Solid Films*,2008,**516**:4325—4329.

(上接第 171 页)

[22] Shu G W, Lee W Z, Shu I J, *et al.* Photoluminescence of colloidal CdSe/ZnS quantum dots under oxygen atmosphere [J]. *IEEE Transactions on Nanotechnology* 2005,**4**:632—636.

[23] Passow T, Leonardi K, Heinke H, *et al.* Quantum dot formation by segregation enhanced CdSe reorganization[J]. *J. Appl. Phys.* 2002,**92**:6546—6552.

[24] Lee W Z, Shu G W, Wang J S, *et al.* Recombination dynamics of luminescence in colloidal CdSe/ZnS quantum dots[J]. *Nanotechnology* 2005,**16**:1517—1521.

[25] Chen X, Lou Y, Samia A C, *et al.* Coherency strain effects on the optical response of core/shell heteronanostructures[J]. *Nano Lett.* 2003,**3**:799—803.

[26] Strassburge M, Dworzak M, Born H, *et al.* Lateral redistribution of excitons in CdSeZnSe quantum dots[J]. *Appl. Phys. Lett.* 2002,**80**:473—475.